

QM/MM As a Tool in Fragment Based Drug Discovery. A Cross-Docking, Rescoring Study of Kinase Inhibitors

M. Paul Gleeson^{*,†} and Duangkamol Gleeson[‡]

Computational & Structural Chemistry, GlaxoSmithKline Medicines Research Centre, Gunnels Wood Road, Stevenage, Hertfordshire SG1 2NY, United Kingdom, Department of Chemistry, Faculty of Science, King Mongkut's Institute of Technology Ladkrabang, Bangkok 10520, Thailand

Received January 17, 2009

The use of QM/MM based methods to optimize and rescore GOLD derived cross-docked protein–ligand poses has been investigated using a range of fragment-like kinase inhibitors where experimental data have been reported. Particular emphasis has been placed on rationalizing the potential benefits of the method in the increasingly popular fragment based drug discovery area. The results of this cross-docking, rescoring study on 9 protein ligand complexes suggest that the hybrid QM/MM calculations could prove useful in kinase fragment based drug discovery (FBDD). B3LYP/6-31G**//UFF derived enthalpies allow us to identify the correct X-ray pose from a range of plausible decoys 77% of the time, almost a doubling of the retrieval rate compared to GOLD (44%). In addition, this method provides us with a means to rapidly and accurately generate virtual protein–ligand complexes that will allow a program team to probe the existing interactions between the ligand and protein and search for additional interactions.

1. INTRODUCTION

Fragment based drug discovery (FBDD) has become an important alternative to traditional high throughput screening (HTS) methods in lead generation.^{1–3} The attractiveness of FBDD is that one can screen relatively small numbers of fragments (~1000 s) at high concentration using biochemical, NMR, or crystallographic methods and obtain higher hit rates compared to conventional HTS campaigns of 1,000,000s of molecules.^{1,2} This is because the probability of observing a useful binding event to a receptor is higher for a small fragment since fewer features need to be matched.⁴ On the other hand, given the reduced number of matched features one can only expect hits of modest affinity. A crucial component of the FBDD method is the use of structural techniques such as NMR and X-ray crystallography which are needed to define the precise binding mode of the low potency fragment hits.^{5,6} Using structure based drug design (SBDD) techniques more potent, druglike ligands can then be synthesized to make additional interactions with other residues in the binding site. Alternatively the method can be used to explore the linking of two or more fragments together which are bound to alternate positions in the binding site.

For FBDD to be successful it is crucial that SBDD techniques are used to follow-up the initial screening efforts, and this is where computational chemistry can prove valuable.^{7,8} Having the ability to theoretically design a selection of new ligands to probe the existing interactions between the ligand and protein as well as search for additional new interactions provides an efficient means to

prosecute a drug discovery program. Key to the success of this endeavor is the accuracy of the computational methods such as docking and scoring. However, these methods have recently come under criticism.^{9–13} It can be concluded that docking programs can generally reproduce the experimental binding modes for a diverse set of targets and ligands; however, the methods cannot presently distinguish the crystallographic conformation from the other poses generated or rank ligands according to their affinity. This is also true for the types of reduced-complexity fragments used in FBDD making the use of computational methods less influential than they could be.¹⁴

To gain wider acceptance in the structure or fragment based drug design, greater effort is needed to develop and validate more sophisticated computational methods that will instill greater confidence.¹⁵ More advanced methods recently reported that look promising include MM-PB/SA,¹⁶ MM-GB/SA,^{17,18} and equivalent QM/MM based versions^{19,20} as well as quantum-polarized-ligand-docking (QPLD).^{21,22} However a criticism of many docking methods is that their performance is often assessed by redocking the ligand into the “native” protein conformation determined for that precise ligand. This represents a best case scenario, unlike in cross-docking where the ligand is docked into a suboptimal protein conformation derived with a different ligand or none at all.^{10,13} This is more representative of the process in lead generation where only biochemical data for a novel hit are available initially.

This study has been designed from the outset to mirror how a computational chemist would support a Lead Identification (LI) program where no structural information is available for the ligand of interest. In this case a protein structure with a different bound ligand is chosen for cross-docking of the ligand of interest, and in most cases the two ligands will be from different chemical series. One of the

* To whom correspondence should be addressed. Current address: Department of Chemistry, Faculty of Science, Kasetsart University, 50 Phaholyothin Rd, Chatuchak, Bangkok 10900, Thailand. Phone: +66-86-5242120. Fax: +66-2-5793955. E-mail: paul.gleeson@ku.ac.th.

[†] GlaxoSmithKline Medicines Research Centre.

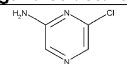
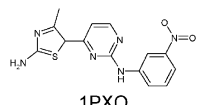
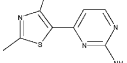
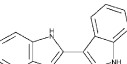
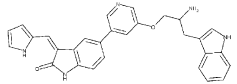
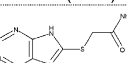
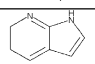
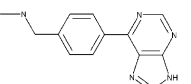
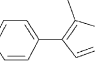
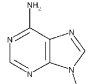
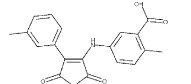
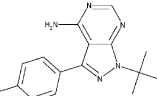
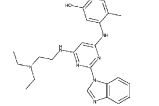
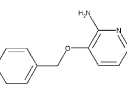
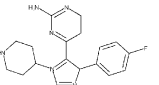
[‡] King Mongkut's Institute of Technology Ladkrabang.

main hurdles in the docking of a new chemotype to a known protein structure are protein conformational effects. These are impossible to predict apriori, so when cross-docking one (A) takes a best guess at the most likely protein conformation, (B) uses multiple structures, or (C) includes a degree of flexibility using methods such as induced fit docking. In practice both options B and C are undesirable in a high throughput screening environment as they are both time-consuming and lead to many more protein–ligand structures to be ranked for a given ligand. In addition, induced-fit methods will not predict domain movements which are the major concern in kinase docking. While option A is also flawed, one typically chooses a protein structure for cross docking based on the ligand (or in-depth structural knowledge of the target), and typically the structure with the most similar ligand is the structure that is chosen. In this study we deliberately choose ligands from distinctly different chemotypes to make the situation more reflective of reality, as rarely does one have a great deal of choice, particularly with novel targets in lead identification. We focus on fragment based inhibitors, which are very much smaller than typical kinase inhibitors on the market, where binding is typically driven by 1 or 2 polar interactions. Thus the impact of large domain or loop movement, will be more limited, especially since the adenine binding pocket is the least perturbed region. This makes them more amenable to rigid receptor docking and QM/MM calculations.

Here we investigate the performance of a novel procedure to theoretically reproduce the X-ray binding conformations of fragment-like inhibitors, relying on GOLD²³ for the cross-docking experiment and QM/MM²⁴ for pose optimization and rescoring. The reason for this study is to try and determine whether computational science has evolved sufficiently such that we can theoretically describe protein–ligand interactions in an accurate, reliable, and timely manner as this would represent a significant breakthrough due to the resource intensive nature of crystallography support.

We focus on inhibitors of kinases given that these represent the largest protein family in humans²⁵ and are believed to account for up to one-third of all drug discovery programs.²⁶ In addition, this target class has been extensively studied using crystallographic methods (~50 unique kinase structures exist²⁷) and have been actively targeted using FBDD efforts.^{1–3} To this end, 9 fragment-like protein–ligand complexes spanning 6 different kinases were obtained from the RCSB protein databank.²⁸ In addition, 6 protein structures for each of the 6 different kinases were also extracted for the cross-docking experiments at random (Table 1). Making the more realistic, these protein structures contain structurally different ligands, and in 3 instances, there exist significant conformational differences compared to the original protein structures. We do not consider redocking to the original reference protein here as this is generally considered to be an unrealistic test and not reflective of real world use.²⁹ A set of plausible cross-docked binding modes for each of the fragment-like inhibitors are generated using GOLD which are then reoptimized using the hybrid QM/MM method, where the inner QM region consists of the ligand and the backbone of 3 amino acids of the so-called hinge, and the remaining protein modeled using MM.³⁰ For the purpose of comparison, the QM region is fully optimized using 3 different levels of theory (B3LYP/6-31G**, HF/3-21G*, and

Table 1. List of the Kinase Protein-Inhibitor Complexes Used in This Study^d

kinase	fragment-like protein ligand structures	cross-docking protein ligand structures
CDK2	 1WCC - (0.5 Å) ^a	 1PXO
	 2C5O ^b - (4.2 Å) ^a	
CHK1	 2C3L - (1.0 Å) ^a	 2GHG
	 2CGX ^b - (1.3 Å) ^a	
PKA/B	 2UVX - (2.5 Å) ^a	 2UVY
	 2UW3 - (0.5 Å) ^a	
GSK3	 1O9U - (4.5 Å) ^a	 1Q4L
LCK / HCK	 1QCF ^c - (5.8 Å) ^a	 2HK5
P38	 1W7H - (1.0 Å) ^a	 1BL7

^a The distance reported in parentheses for the fragment-like structures is the rmsd of the main chain protein heavy atoms to those of the cross-docking structure. ^b This indicates where significant protein domain movement impacts on the active site region. ^c This refers to the fact that HCK and LCK have comparatively high homology (~99%); however, there are some distinct differences in the active site. Both factors would be expected to complicate the cross-docking studies. ^d Protein structures derived from the inhibitors on the right were used for the cross-docking experiments of the corresponding inhibitors on the left.

PM3), and the MM region is treated using the Universal Force Field (UFF).³¹ The docking poses for each ligand are then ranked according to the predicted QM/MM enthalpy. In the ONIOM based implementation used here^{32,33} the total QM/MM energy is computed as the QM energy of the inner region including the MM charges, plus the MM energy of the whole outer region, minus the MM energy of the inner region (eq 1). For further details of the QM/MM method used here see ref 30. For additional reviews discussing the application of the QM and QM/MM methods see refs 34 and 35.

$$E_{\text{QM/MM}} = E_{\text{inner}}^{\text{QM+MMcharges}} + (E_{\text{outer}}^{\text{MM}} - E_{\text{inner}}^{\text{MM}}) \quad (1)$$

The QM/MM results are subsequently contrasted with those obtained: (a) using the empirical docking score derived from GOLD and (b) using the energy of docked complexes where the docked ligand conformation has been reoptimized using the Merck Molecular Force Field (MMFF).³⁶ The ultimate goal of this study is to see if, under identical conditions, more advanced theoretical methods offer any advantage over computationally less demanding empirical methods.

2. COMPUTATIONAL PROCEDURES

Protein Preparation. The 15 X-ray crystal structures (9 native + 6 non-native) downloaded from the RCSB protein databank were prepared as follows (Table 1). Cofactors, ions, and water molecules were removed from the protein–ligand complexes as these can be ligand specific and could thus interfere in cross-ligand docking experiments being undertaken here.³⁷ Each protein was prepared using the protein preparation wizard in Maestro.³⁸ Hydrogen atoms were added to the system, and ionizable amino acid side chains were protonated assuming a pH of 7.4. The 6 non-native protein structures underwent restrained minimization using the IMPREF utility,³⁸ to optimize hydrogen atoms and to remove any high energy contacts or distorted bonds, angles, and dihedrals. These protein coordinates were used for the subsequent GOLD cross-docking experiments. IMPREF restrained minimization led to negligible changes in the active site region, being used to remove high energy amino acid defects if present.

Ligand Preparation. The 2D smiles of the 9 ligands required for cross-docking were converted into 3D coordinates using the Ligprep³⁸ module in Maestro. The ligands were optimized using the MMFF forcefield in Macromodel,³⁸ and the coordinates were saved in mol2 format for use in GOLD.

GOLD Docking Procedure. Ligands were cross-docked into the appropriate non-native protein structure listed in Table 1. The active site of the non-native protein structure was defined using the original ligand. To minimize the number of spurious docking solutions generated by GOLD a restraint was added such that a pose was only accepted if a H-bond existed between any acceptor atom on the ligand and the H-bond donor of the hinge. This restraint is not unreasonable given this interaction is present in almost all kinase inhibitors.²⁷ The GOLD program was executed using the “diverse conformer selection” option switched on and the “no early termination” option off to generate as many poses as possible for each ligand. Ten diverse conformations were archived for each ligand.

The GOLD conformations for each ligand were clustered, and the highest ranked GOLD score pose from each was selected for further analysis. Two to 3 conformers for each ligand were selected for QM/MM and MM rescoring.

Reference Structure Generation. An additional ligand reference structure was generated for each ligand by aligning each of the native and non-native protein pairs in Table 1 based on their C α s. The ligand was extracted from the former and inserted into the latter as this represents our best guess. It also allows us to assess the affect of the conformational differences between the two proteins. This pose is henceforth termed the reference structure, conformer or pose.

QM/MM and MM Rescoring. All cross-docked protein–ligand complexes were optimized using the ONIOM methodology developed by Morokuma and co-workers,^{32,33} as implemented in Gaussian 03.³⁹ We have employed our previously described model,³⁰ with a QM region consisting of the bound ligand and the backbone of the 3 amino acids of the hinge, and the point charges of the outer MM region being electrically embedded within the SCF calculation. Where bonds cross the QM and MM interface, the valences were satisfied by hydrogen link atoms. In this case the outer region is kept fixed, and the charges are assigned using the charge equalization method.⁴⁰ The latter method has been demonstrated to produce molecular charges that correlate well with more expensive QM calculations. The inner QM region was treated using a range of different levels of theory: B3LYP/6-31G**, HF/3-21G*, and PM3. Electrical embedding was used in all cases apart from PM3, where mechanical embedding was used as the latter is not supported. The van der Waals contribution to the protein–ligand complexes was treated classically using the universal force field (UFF)⁴¹ as implemented in Gaussian 03. This combination has been applied successfully in the past for calculations on protein-kinase complexes³⁰ and large representations of 3-dimensional zeolites catalysts.^{42–44} We restrict the QM portion of the calculation to three amino-acid backbones, corresponding to the hinge region of the adenine binding pocket (containing the acceptor, donor, acceptor feature) as this is the key binding partner of most kinase inhibitors. Since we are dealing with a small, rigid fragment, it is reasonable to encode the more distant van der Waals components classically, with the electrostatic contribution estimated by embedding the atomic charges in the QM calculation. The total QM/MM energy of the protein–ligand complex is used to rank the ligands, the lower the value (Kcal/mol) the better, unlike the GOLDScore which increases.

The QM theory and basis sets explored in this study were chosen to span the relatively quick (PM3) to the relatively slow (B3LYP/6-31G*). While more advanced methods incorporating electron correlation such as MP2 would be preferred, such calculations are competing with the MM methods that give near instantaneous results, so they have not been pursued here. B3LYP has shown good correlation with experimental data in many applications and is an accepted standard in calculations on proteins. Examples include refs 19, 30, and 45. Gaussian 03 calculations were submitted as single processor jobs on a linux cluster and took no more than 2 days to converge.

The cross-docked protein–ligand complexes were also assessed using forcefield methods for the purpose of comparison. In this case the whole protein was fixed, and the ligands were optimized using MMFF⁴⁶ as implemented in MOE.⁴⁷ More effective force field methods such as AMBER⁴⁸ or CHARMM⁴⁹ were not considered due to the time-consuming setup required for each ligand. As with the QM/MM methods, the total MM energy of the protein–ligand complex is used to rank each pose.

rmsd Calculation. For each of the theoretically derived ligand conformers we compute the rmsd to the original native crystal structure ligand pose. We use a 1 Å rmsd cutoff in this study to define the true binding mode as well as visual confirmation. This is due to the size of the ligands under investigation and because the more commonly used 2 Å

Table 2. GOLD Docking Results for the 9 Protein-Inhibitor Complexes^c

kinase	ligand	GOLD solution	GOLD score ^a	rmsd	pose comment
CDK2	1WCC	1	25.8	2.4	2HBs inner/central
		2 (X-ray)	24.6	0.5	1HB central
		5	22.8	3.7	2HBs outer/central
	2C5O	1	39.2	5.0	1HB central (via thiazole N)
		4 (X-ray)	36.7	0.8	2HBs outer/central
CHK1	2C3L	5	36.6	2.1	2HB to outer/central (incorrect thiazole rotamer)
		1 (X-ray)	48.4	0.6	3HBs inner/central/outer
		2	46.5	1.3	2HBS inner/central (benzimidazole-rotamer)
	2CGX	3	42.2	4.6 (2.6)	2HBs inner/central (via pyridyl-imidazole)
		6	40.3	3.1 (2.5)	2HBs inner/central
PKA/B	2UVX	7 (~X-ray) ^b	39.9	2.4 (1.8)	2HBs outer/central
		1 (X-ray)	36.4	0.5	2HBs inner/central
		2	32.4	3.5	2HBs outer/central
	2UW3	1 (X-ray)	42.0	0.1	2HBs inner/central
		8	38.6	3.4	2HBs outer/central
GSK3	1O9U	1	27.0	3.6	2HBs outer/central
		5 (X-ray)	26.4	0.9	2HBs inner/central
		10	25.5	2.6	1HB center
HCK/LCK	1QCF	1	48.1	2.1	2HBs inner/central
		4 (X-ray)	40.1	0.9	2HBs inner/central
P38	1W7H	1 (X-ray)	45.1	0.5	2HBs inner/central
		5	33.1	3.5	2HBs inner/central (phenyl to solvent)

^a The GOLD score is reported in arbitrary units with a larger value corresponding to a lower overall energy. ^b The template correctly docked apart from the amide substituent due to protein conformational differences in non-native structure. ^c Only results for the top ranked, unique poses are reported. Listed are the ranking of the GOLD solution, the GOLD score, the overall RMSD to the reference crystallographic coordinates, and a brief description of the pose.

cutoff can be met by very different binding modes. We only use this parameter in a qualitative fashion given that its use as a metric to decide the success of docking experiments has come under criticism recently.^{50,30} This is because a crystal structure is itself a fitted atomic model derived from the electron density, solved using empirical methods in an iterative manner to best fit, what can often be ill-defined density, particular for more mobile ligands. In fact it has been reported that the atomic positional errors for crystallographic structures with resolutions between 1.8–2.0 Å will range from ~0.2–0.3 Å.^{51,52} Thus its use as an absolute comparator is unjustified.

3. RESULTS

3.1. GOLD Docking Results. For 1WCC 3 unique cross-docked protein–ligand complexes required rescoring, along with 3 for 2C5O, 2 for 2C3L, 3 for 2CGX, 2 for 2UVX, 2 for 2UW3, 3 for 1O9U, 2 for 1QCF, and 2 for 1W7H (Table 2). Taking 1WCC as an example, from Table 2 we can see that solution-1 is a conformation where the docked ligand makes two H-bonds to the hinge, one to the inner acceptor and another to the central H-bond donor. The second ranked GOLD solution is also unique, corresponding to the X-ray conformation. Here the ligand makes a single H-bond to the central donor of the hinge. The next nonredundant solution is not obtained until the fifth ranked pose is reached. Here the docked conformation makes 2 H-bonds, one to the central donor and, this time, one to the outer H-bond acceptor, not the inner.

In all but one case (2CGX) GOLD was able to reproduce the X-ray conformation (defined here as a root-mean-square deviation (rmsd) <1 Å) in the non-native protein due to significant conformational differences observed between it and the native protein within the glycine rich loop region. The amide group of the ligand is unable to form 2 H-bonds

to the glycine rich loop in the former structure, instead forming an interaction with glutamic acid at the mouth of the ATP binding site. In contrast, noticeable shifts in the glycine rich loop for 2C5O did not result in as significant an issue with the docking solutions. Similarly, docking the ligand from the LCK complex 1QCF, into the protein structure of HCK (2HK5), a protein with ~99% homology in the kinase domain results in a surprisingly good pose with an rmsd of ~0.9 Å, especially given the more constricted ATP cavity in the latter due to the glycine-loop shift.

Thus, in eight of the 9 cases GOLD was able to produce a conformation within 1 Å of the X-ray conformation. However, analysis of the results in Table 2 shows that the GOLD score was only able to discriminate the X-ray conformations from the decoys in 4 out of 9 cases, representing a rather poor 44% success rate (i.e. ranking the correct solution as the top pose). We have only used the standard GOLD scoring function as numerous studies have demonstrated that a range of scores show the same rather low predictivity.⁹

3.2. QM/MM and MM Rescoring Results. The 22 GOLD derived protein–ligand docked complexes in Table 2 were subsequently reoptimized and rescored using both QM/MM and MM. In addition, the nine so-called reference cross-docked structures were also investigated, these having been generated by aligning the native and non-native protein–ligand crystal structures based on their protein C_αs. These references could be considered to represent a best case docking to the non-native protein. Thus, a total of 31 non-native protein–ligand complexes were rescored using 4 different methods, with the results using B3LYP/6-31G**//UFF, HF/3-21G**//UFF, PM3//UFF, and MMFF in Table 3. For brevity during the discussion these results are referred to as the QM/MM-DFT, QM/MM-HF, QM/MM-PM3, and MMFF, respectively. In addition to the tabulated results, an

Table 3. QM/MM and MM Results for the Reoptimized GOLD Cross-Docked Structures and Reference Structure^f

kinase	ligand	GOLD pose rank	B3LYP/6-31G**//UFF		HF/3-21G**//UFF		PM3//UFF		MMFF	
			energy	rank	energy	rank	energy	rank	energy	rank
CDK2	1WCC	1	6.5	2	14.7	2	0.0	1	0.6	2
		2 (X-ray)	0.0	1 ^a	0.0	1 ^a	0.1	2 ^b	0.0	1 ^a
		5	21.2	3	17.0	3	12.6	3	3.3	3
	2C5O	-	3.0	reference	3.0	reference	6.2	reference	0.0	reference
		1	10.5	3	20.2	3	14.1	3	0.0	1
		4 (X-ray)	4.8	2 ^b	5.3	2 ^b	10.1	2 ^b	0.7	2 ^b
CHK1	2C3L	5	0.0	1	0.0	1	8.5	1	11.4	3
		-	9.8	reference	6.5	reference	0.0	reference	11.4	reference
		1 (X-ray)	0.0	1	0.0	1 ^a	0.0	1 ^a	0.0	1 ^a
	2CGX	2	17.8	2	23.6	2	10.8	2	8.6	2
		-	3.6	reference	3.6	reference	3.5	reference	5.0	reference
		3	0.0	1	3.8	2	0.0	1	12.9	1
PKAB	2UVX	6	53.9	3	37.4	3	31.4	3	21.5	2
		7 (~X-ray) ^c	18.0	2 ^b	0.0	1 ^d	23.1	2 ^b	21.5	2 ^b
		-	89.6	reference	62.8	reference	47.1	reference	0.0	reference
	2UW3	1 (X-ray)	0.0	1 ^a	0.0	1 ^a	0.0	1 ^a	0.0	1 ^a
		2	13.9	2	17.0	2	10.5	2	10.9	2
		-	0.1	reference	0.0	reference	0.9	reference	0.0	reference
GSK3	1O9U	1 (X-ray)	0.0	1 ^a	7.4	2 ^b	0.8	2 ^b	0.0	1 ^e
		8	12.5	2	0.0	1	0.4	1	0.0	1
		-	7.3	reference	0.8	reference	0.0	reference	0.0	reference
	1QCF	1	0.9	2	0.0	1	0.0	1	0.0	1
		5 (X-ray)	0.0	1 ^a	0.9	2 ^b	9.7	3 ^b	6.9	2
		10	19.0	3	20.6	3	8.4	2	15.4	3 ^e
P38	1W7H	-	4.1	reference	5.1	reference	8.4	reference	6.9	reference
		1	12.5	2	12.6	2	13.5	2	0.0	1
		4 (X-ray)	9.5	1 ^a	9.9	1 ^a	10.2	1 ^a	12.2	2 ^b
	1W7H	-	0.0	reference	0.0	reference	0.0	reference	0.6	reference
		1 (X-ray)	0.0	1 ^a	0.0	1	0.0	1 ^a	0.0	1 ^a
		5	23.4	2	23.8	2 ^b	12.0	2	15.5	2
		-	3.1	reference	3.1	reference	2.8	reference	0.0	reference

^a Top ranked docking pose corresponds to X-ray conformation. ^b X-ray conformation not ranked as the top pose. ^c The template is correctly docked but not the amide substituent due to protein conformational differences in the non-native structure. ^d The HF method for 1O9U might only be considered a partial success as the amide substituent conformation cannot be reproduced in the non-native protein. ^e Both poses are equivalently ranked so the method is unable to distinguish decoy from true pose. ^f Reported for each pose are the corresponding relative QM/MM energies (kcal/mol), the new QM/MM rank with respect to the total number of unique GOLD conformers, and a comment field noting which pose represents the crystal structure. The reference pose refers to a pose generated from the alignment between the native and non-native protein structures.

illustration of the lowest rmsd cross-docked, reoptimized pose for each ligand is reported. In Figure 1 the results are reported for cases where the protein conformational differences between the non-native and native structures are small. In Figure 2 the results are reported for those examples where the protein conformational differences between the non-native and native structures are large.

1WCC. The QM/MM-DFT method is able to correctly identify the true binding mode from the 2 decoys unlike the empirically derived GOLD score. Here we define success as obtaining a pose in the non-native structure that is within ~1 Å of that observed in the native structure. Interestingly, the correct cross-docked pose is ~3 kcal/mol lower in energy compared to the optimized reference conformation suggesting the GOLD derived solution is closer to the minimum energy conformer in the non-native structure than the structural alignment pose. In addition, the correct GOLD generated pose is considerably lower in energy than the next lowest energy GOLD decoy pose at ~7 kcal/mol giving us confidence that the former mode is likely to dominate over the other possibilities.

The results obtained using the QM/MM-HF method are also successful in discriminating the equivalent X-ray pose from the decoys, as is MMFF, but not the intermediate QM/MM-PM3. Even though the equivalent X-ray conformation

is just 0.1 kcal/mol higher in energy than the lowest energy decoy using the latter method, it must still be classed a failure since at best an equivocal result will require additional experimental input to resolve the ambiguity.

2C5O. None of the theoretical methods rank the cross-docked pose corresponding to the X-ray binding mode as the lowest energy solution. As mentioned in the previous section, this result is in part due to significant loop movement observed in the non-native protein structure, which can be appreciated by considering the theoretical results to the original, unoptimized native protein–ligand complex (Figure 2). Optimization of the reference in the non-native protein using the QM/MM-DFT method leads to an energy ~10 kcal/mol above the lowest ranked pose and ~5 kcal/mol above the equivalent GOLD derived X-ray equivalent pose.

This result highlights the difficulties experienced when docking is performed in cases where protein flexibility is sizable, and this might have been predicted beforehand given the considerable size difference between the ligands from the native and non-native structures (Table 1). Furthermore, such failures could be mitigated against based on the findings of Sutherland et al.¹⁰ who report that the protein complexes containing the structurally most similar ligand should be used where possible for cross-docking studies.

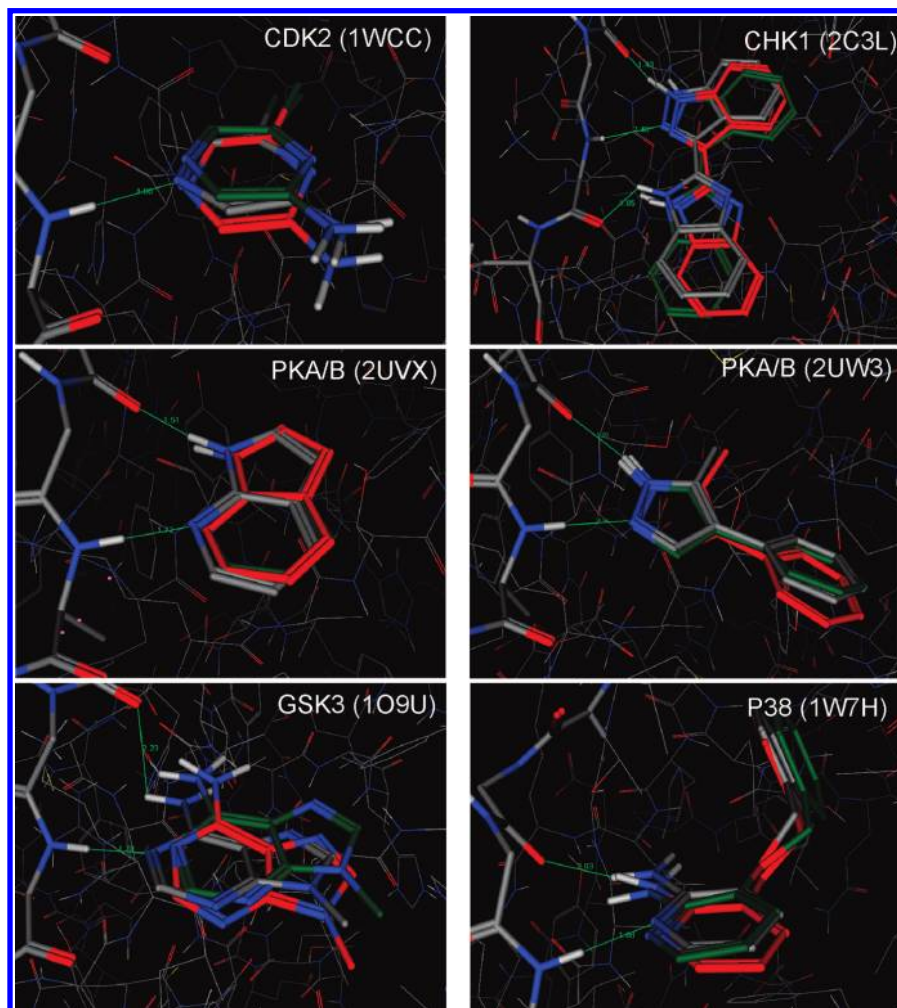


Figure 1. Illustration of the lowest rmsd cross-docked protein-inhibitor solution derived from GOLD (gray) and the reoptimized ligand coordinates at the B3LYP/6-31G**//UFF (red). Also illustrated for the purpose of comparison are the original ligand crystallographic coordinates, superimposed into the cross-docking protein structure based on the alignment of their protein C α s (green).

2C3L. All theoretical methods are able to discriminate between the experimentally known binding pose and the decoys generated in the non-native protein. The QM/MM-DFT results in Table 3 predict the difference in energy between the two lowest energy poses being ~ 18 kcal/mol giving us confidence that the lowest energy pose is significantly lower in energy, and we can thus have greater trust in the results. This is in contrast to the empirically derived GOLD score where the predicted difference is just 1.9 arbitrary units. This rather small difference cannot inspire as much confidence that the two poses are truly different, in contrast to the more rigorous QM/MM-DFT result.

2CGX. As a result of sizable conformational changes in the glycine rich loop none of the conformations obtained during the docking process were particularly close to the original X-ray conformation. This was because the ligand was capable of forming 2 H-bonds with the glycine rich loop in the non-native protein (Figure 2). Nonetheless, the adenine template can H-bond to the hinge in a number of ways (Table 2), so one can still assess whether the methods will identify the correct bonding pattern. It is found that only the QM/MM-HF method correctly identifies the experimental H-bonding pattern to the hinge. However, given that it will be shown that it is not the most accurate method overall it may simply be a fortuitous result given.

It is also worth noting that the QM/MM-DFT non-native reference structure is highly destabilized compared to the lowest energy non-native pose by ~ 90 kcal/mol, and this again highlights the negative impact of protein flexibility on structure prediction.

2UVX. For UVX all of the theoretical methods are able to discriminate between the experimentally known binding pose and the decoys generated in the non-native protein. In Table 2 one can also see that the QM/MM-DFT energies for the GOLD derived X-ray pose and the alignment derived reference are 0.0 kcal/mol highlighting that the conformational differences between the native and non-native structures are rather minor (Figure 1). This might be expected given the common core of the ligands from the native and non-native proteins (Table 1).

2UW3. The non-native pose of 2UW3 that corresponds to the X-ray conformation is predicted to have the lowest energy according to QM/MM-DFT method and the GOLD-score only. The difference in energy between the correct pose and decoy poses is substantial at ~ 13 kcal/mol using the former method giving us confidence that the difference is meaningful. The MMFF based method predicts the two different poses as having equivalent energies, while the value is just 0.4 Kcal/mol for QM/MM-PM3 but 7.8 Kcal/mol using the QM/MM-HF method. We still consider the QM/

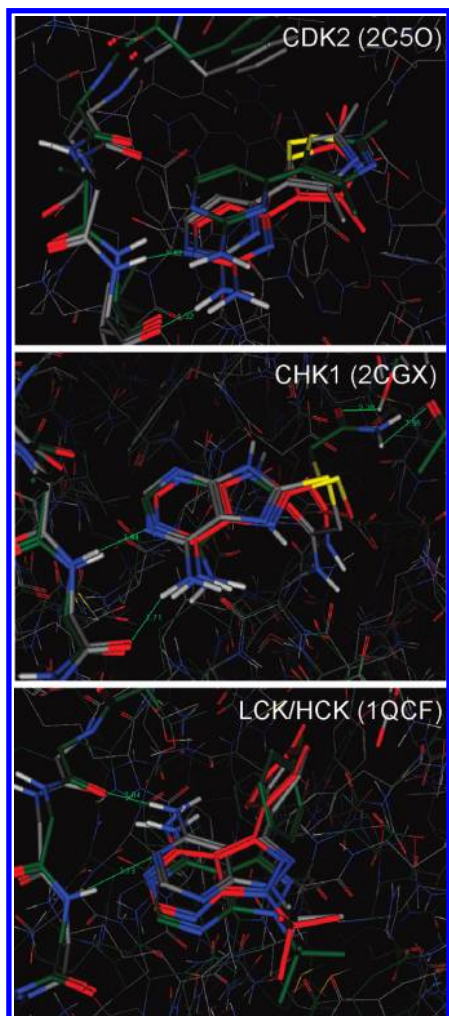


Figure 2. Illustration of the results for those examples where conformational differences in the cross-docking protein structure are significant. Details are the same as for Figure 1.

MM-PM3 and MMFF results to be failures since equivocal result requires additional experimental input to resolve the ambiguity.

1O9U. For 1O9U only the QM/MM-DFT method is able to differentiate the true cross-docked X-ray pose from the 2 other decoys. This difference is predicted to be rather small at just 0.9 kcal/mol which does not inspire significant confidence in the result. This is perhaps a reflection of the low resolution data of 1O9U (2.4 Å). Alternatively the ambiguous electron density observed for the ligand, which we have already commented on elsewhere,³⁰ may simply be a result of sampling a number of relatively low energy, accessible conformations during the time-course of the experiment. This would help to explain the theoretical result obtained.

1QCF. In this rather difficult case we have cross docked a ligand found in HCK into the closely related protein structure of LCK. The results obtained using the QM/MM-DFT, QM/MM-HF, and QM/MM-PM3 methods are successful in identifying the expected X-ray binding mode from the decoy poses in the non-native protein structure. In contrast, MMFF rescoring and the GOLD score cannot discriminate between the true and decoy poses.

The QM/MM-DFT optimized reference conformation is lower in energy than the equivalent GOLD derived X-ray

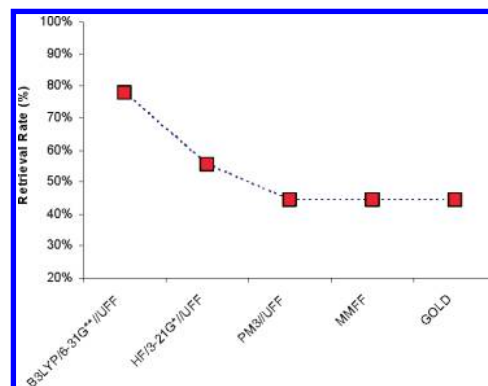


Figure 3. % of cases for each method where the top ranked cross-docked structure corresponded to the crystallographic pose (% retrieval rate). Percentages are based on a total of 9 examples.

conformation (9.5 Kcal/mol), suggesting the latter did not do a particularly good job in docking the ligand. This difference can be appreciated from Figure 2 where it can be seen that starting from an alignment-derived pose will lead to an alternate conformation where the phenyl ring rotamer will be more ideal. The incorrect GOLD rotamer may be a result of a subtle movement of the catalytic aspartate and lysine residues altering the shape of the binding pocket and the reduced van der Waals cut-offs used during the docking procedure.

1W7H. For the final protein–ligand complex considered here, 1W7H, two possible poses were generated in the cross-docking study using GOLD, and all methods are able to discriminate between the d X-ray pose and the decoy.

The combined results obtained from the QM/MM and MM rescoring exercise are summarized in Figure 3. For fragment-like kinase inhibitors at the very least, the results indicate the benefits of using accurate QM/MM methods to reoptimize and rescore the output from more simplistic empirical docking programs such as GOLD. In 77% of the examples studied here (7/9 cases) the B3LYP/6-31G**//UFF method was able to correctly identify the true X-ray pose from the decoys, simply using the total QM/MM enthalpy as the discriminator. The HF/3-21G*//UFF based result was the next most effective, having a 66% retrieval rate, or ~60% (6/9) if the 2CGX result is only considered a partial success (5.5/9). The semiempirical QM/MM-PM3 based method offers no advantage over GOLD and nor does the MMFF rescoring, as demonstrated by the equivalent retrieval rates of 44% (4/9).

In the two cases where the QM/MM-DFT method failed, significant conformational differences were observed between the native and non-native protein conformations which led to confounding effects (2CGX and 2C5O). In cases where the RMSDs between the native and non-native protein main chains were >2.0 Å (1QCF, 1O9U, 2UVX), but did not necessarily impact the active site so significantly, the DFT QM/MM method was able to identify the correct binding mode as the top ranked solution indicating a degree of robustness in the method. For very small fragments, it is understandable that protein conformational effects do not have as significant a detrimental effect on our ability to identify the true binding mode from the decoys. Here, we observe the QM/MM DFT method to be successful for small fragments even in cases where the RMSDs between the native and non-native protein main chains differ significantly:

Table 4. Summary of the Reoptimized GOLD Protein-Ligand Structure with the Lowest Overall RMSD^a

kinase	ligand	B3LYP/6-31G**//UFF				HF/3-21G**//UFF			
		rank	rmsd	HB1	HB2/3	rank	rmsd	HB1	HB2/3
CDK2	1WCC	1/3	0.55 (0.53)	2.08	-	1/3	0.57 (0.56)	2.02	-
	2C5O	2/3	1.11 (1.08)	1.83	1.89	2/3	1.07 (0.99)	1.78	1.83
CHK1	2C3L	1/2	0.66 (0.67)	2.08	1.91/1.72	1/2	0.56 (0.57)	2.08	1.80/1.71
	2CGX	2/3	4.98 (1.07)	2.05	1.86	2/3	4.98 (0.79)	2.03	1.83
PKA/B	2UVX	1/3	0.31 (0.36)	1.94	1.74	1/3	0.30 (0.37)	1.91	1.72
	1uw3	1/2	0.42 (0.42)	1.96	2.01	2/2	0.39 (0.38)	1.93	1.95
GSK3	1O9U	1/3	0.83 (0.84)	2.18	1.72	2/3	0.82 (0.83)	2.16	1.69
HCK/LCK	1QCF	1/2	1.38 (1.07)	2.14	1.84	1/2	1.39 (1.11)	2.11	1.85
P38	1W7H	1/2	0.58 (0.64)	1.91	1.97	1/2	0.65 (0.73)	1.89	1.99

kinase	ligand	PM3//UFF				MMFF			
		rank	rmsd	HB1	HB2/3	rank	rmsd	HB1	HB2/3
CDK2	1WCC	2/3	0.60 (0.57)	1.89	-	1/3	0.73 (1.01)	2.35	-
	2C5O	1/3	1.10 (0.94)	1.84	1.82	2/3	0.94 (1.36)	1.65	1.53
CHK1	2C3L	1/2	0.50 (0.50)	2.31	1.89/1.81	1/2	0.75 (0.61)	2.61	1.66/1.35
	2CGX	2/3	4.93 (0.93)	1.83	1.82	2/3	2.60 (0.84)	3.28	3.83
PKA/B	2UVX	1/3	0.29 (0.35)	1.86	1.78	1/3	0.26 (0.30)	1.88	1.66
	2UW3	2/2	0.42 (0.37)	1.87	1.93	2/2	0.32 (0.32)	1.76	1.96
GSK3	1O9U	2/3	0.93 (0.66)	1.92	1.80	2/3	0.82 (0.84)	1.77	2.23
HCK/LCK	1QCF	2/2	1.31 (0.79)	2.32	1.86	2/2	1.37 (0.95)	2.21	2.15
P38	1W7H	1/2	0.67 (0.73)	1.86	2.29	1/2	0.71 (0.79)	1.74	1.91

kinase	ligand	GOLD				X-ray			
		rank	rmsd	HB1	HB2/3	rank	rmsd	HB1	HB2/3
CDK2	1WCC	2/3	0.46	1.98	-	-	-	2.11	-
	2C5O	2/3	0.78	1.49	1.32	-	-	1.84	1.92
CHK1	2C3L	1/2	0.63	2.36	1.65/1.43	-	-	2.17	1.72/1.54
	2CGX	3/3	3.02	2.44	1.71	-	-	1.80	2.56
PKA/B	2UVX	1/2	0.47	1.71	1.72	-	-	1.93	1.98
	2UW3	1/2	0.19	1.99	1.91	-	-	1.92	1.87
GSK3	1O9U	2/3	0.87	2.23	1.78	-	-	2.24	1.82
HCK/LCK	1QCF	2/2	1.40	2.73	2.04	-	-	2.02	2.04
P38	1W7H	1/2	0.49	1.86	2.03	-	-	2.06	2.04

^a The overall pose rank for each method and the total number of poses are reported along with the RMSD to the original crystallographic coordinates and the H-bond distances between the inhibitor acceptor and the central hinge donor (HB1) and the inhibitor donor and hinge acceptor (HB2=inner/HB3=outer). Also reported are the H-bond distances derived from the original X-ray structure where hydrogens have been added using MOE.

1WCC (0.5 Å), 2UVX (2.5 Å), and 1O9U (4.5 Å) suggesting the approach is particularly suited to kinase FBDD. As reported by Sutherland et al.¹⁰ one can mitigate against protein conformational effects by choosing more complementary protein–ligand complexes for the cross-docking studies, where the template is reasonably shape or feature similar.

3.3. QM/MM Structure Prediction. It is reasonable to argue that the QM/MM-DFT method is more effective at discriminating the experimentally determined X-ray poses from the decoys because it represents a phenomenologically precise description of the binding event when compared to the other less demanding methods. To understand whether this might be true or not we now assess how the different theoretical structures compare to the experimentally determined crystallographic coordinates (Table 4 and Figure 4). Since the QM/MM-DFT and QM/MM-HF results closely track in terms of structure we only discuss the former for brevity.

First, we look at the rmsd between the native protein–ligand complex and the equivalent cross-docked protein–ligand complex from each of the theoretical methods (Figure 4). The results show that for all but one of the ligands studied here, we observed the RMSDs to lie below

the commonly used 2 Å cutoff often used to classify a docking as being successful.¹⁰ The results also indicate that the more accurate QM/MM methods do not demonstrate any lower RMSDs than the GOLD conformers from which they were derived. In fact the average rmsd for GOLD is 0.92 Å, compared to 1.20 Å for QM/MM-DFT, 1.20 Å for QM/MM-PM3, and 0.94 Å for MMFF. However, this one-dimensional parameter does not necessarily mean the GOLD or MMFF conformers are more representative of the experimental structures as recently highlighted by Yusuf et al.⁵³

It is interesting to note that if the alignment derived reference conformer rather than the best GOLD derived conformer is taken and optimized in the non-native protein, then the rmsd is on average lower (0.62 Å versus 0.74 Å at QM/MM-DFT). However the reference derived structures are typically higher in energy compared to the equivalent GOLD pose (~3.6 kcal/mol on average at QM/MM-DFT) meaning that the lowest rmsd pose is not necessarily the lowest energy in a non-native protein due to subtleties in the protein conformation which has an impact on ligand strain energy. This leads us to believe that it is better to compare structural parameters that are indicative of the strength of interaction with the protein,

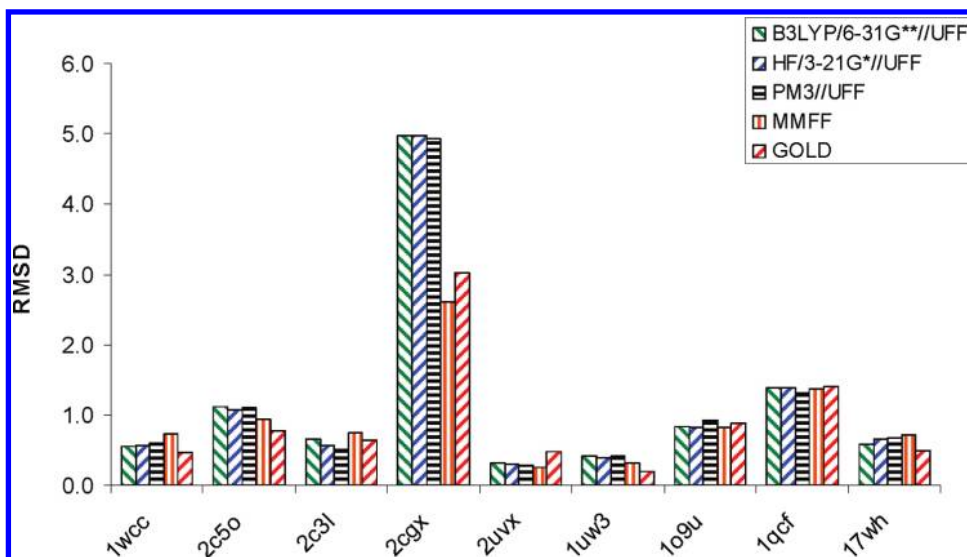


Figure 4. Plot of the rmsd to the native crystal structure for the lowest rmsd, cross-docked theoretical models. Note these do not always correspond to the lowest energy structures as can be determined from Table 3.

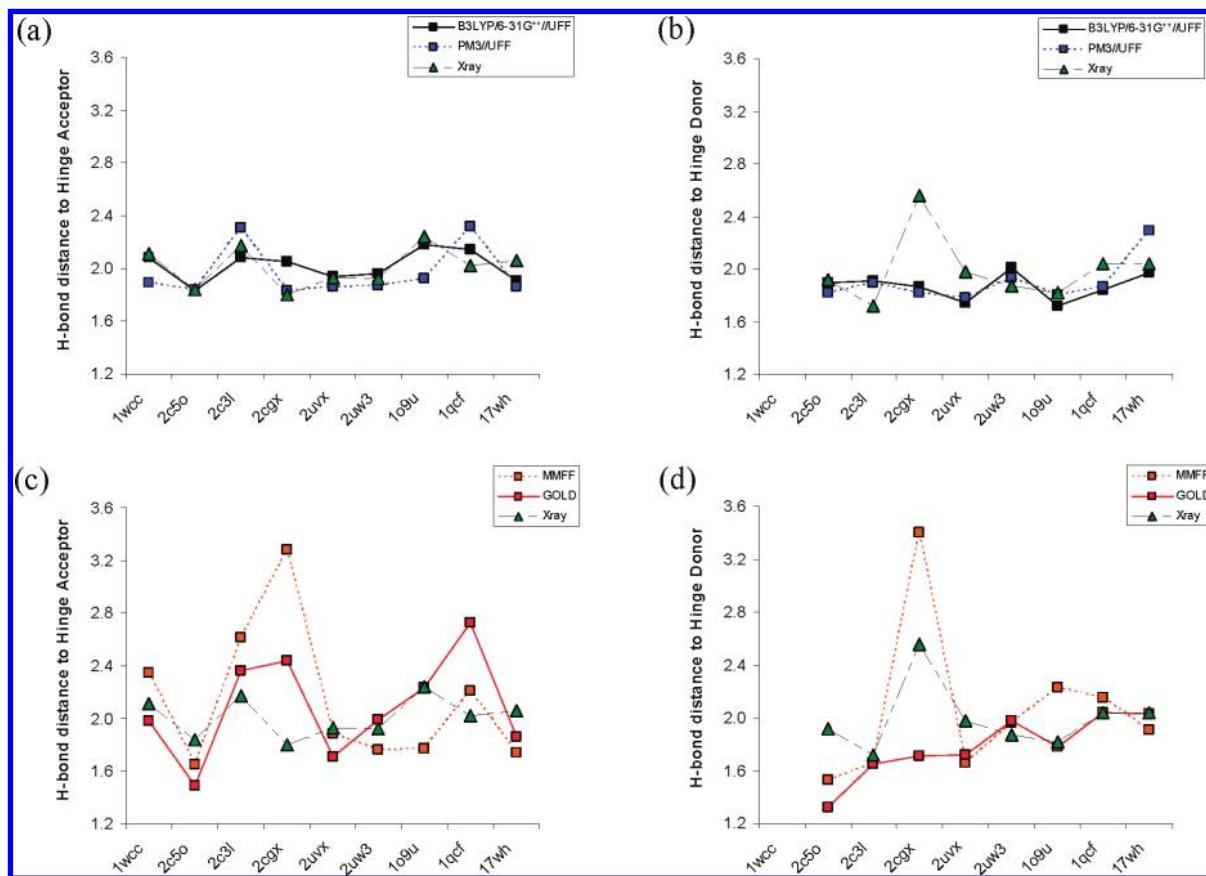


Figure 5. Figure of the H-bond distances derived from the 9 lowest rmsd, cross-docked theoretical models and the corresponding X-ray values. (a and c) show the distance between the ligand acceptor and the hinge donor, and (b and d) show the distance between the ligand donor and either the inner or outer hinge acceptor. For 2C3L only the central and inner H-bond are plotted. HF/3-21G* results are omitted for clarity as they track closely with the DFT and PM3 values.

such as the H-bond distances, as the rmsd can be misleading.^{30,53}

The H-bond distances predicted between the ligand and the hinge are illustrated graphically in Figure 5 for the different methods studied here. We find that the mean H-bond distances between the ligand acceptor and the hinge donor are all comparable being 2.0 Å for the X-ray structure, 2.0 Å using the QM/MM-DFT model, 2.0 Å for QM/MM-PM3, 2.1 Å for GOLD, and 2.1 Å for MMFF.

However it is clear from a visual inspection of Figure 5 that the QM/MM-DFT and QM/MM-PM3 based methods show cross-docked, optimized complexes that track more closely with the H-bonding pattern observed in the native X-ray structure. Apart from 2CGX, the vast majority of H-bonds lie between 1.8–2.2 Å, corresponding to conventional H-bond lengths. In contrast the results derived from the empirical methods GOLD and MMFF are much more variable. The H-bond distances observed range from

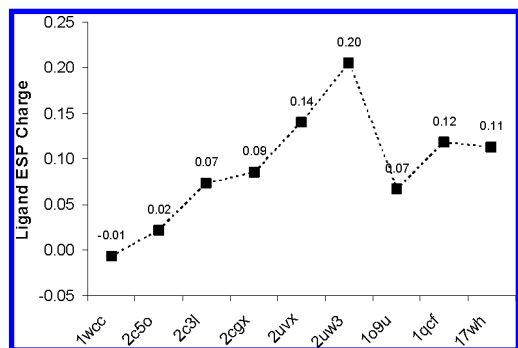


Figure 6. Figure of the total B3LYP/6-31G** ESP charge on the heavy atoms of the formally neutral ligands for the lowest rmsd cross-docked complex.

an unnatural 1.4–3.2 Å, often deviating significantly from the original X-ray structures.

These findings suggest that the structures obtained from empirical or force-field methods such as GOLD and MMFF, while of low rmsd, are often physically unreasonable with less than ideal H-bond distances and that this might help to explain the poor performance of MM scoring functions generally observed in the literature. Interestingly, PM3 demonstrates a quite poor retrieval rate of the X-ray poses here (44%) yet shows rather good agreement with experiment in terms of the H-bonding pattern. This suggests that even the relatively rigorous semiempirical energy description is not sufficiently accurate to allow us to describe the subtle energetic differences in the protein–ligand complex.

Finally, to highlight why one needs more sophisticated computational methods to describe such complex biological systems we consider the important effect of protein electrostatics⁵⁴ on the active site as modeled here. In many force field methods, such as AMBER or CHARMM, amino acids residues, metal ions, and ligands have integer charges; however, the situation is quite different in reality due to the polarizing effect of the protein environment. To illustrate this effect we have calculated the ESP charges on the QM atoms of our system at the B3LYP/6-31G** level and calculated the average electron density observed on the ligand. It is apparent from the results presented in Figure 6 that a significant degree of electron density is transferred from the former to the latter (~ 0.1 A.U. on average), comparable with results of Raha et al.²⁰ These subtleties have implications for the binding energy and are completely neglected by the standard force-fields methods.³⁶

4. CONCLUSIONS

In this study we have investigated the performance of a range of QM/MM based models to reoptimize and rescore GOLD derived cross-docking poses of 9 fragment-like inhibitors, derived from 6 different protein kinases. The results indicate that the most accurate B3LYP/6-31G**/UFF model used here was able to identify the correct binding mode from a range of plausible decoys 77% of the time, almost a doubling of the retrieval rate compared to GOLD alone (44%). In the two cases where the method failed this was attributed to sizable differences between the native and non-native protein structures used for the cross-docking studies. This has implications for larger ligands as relatively

minor changes around the active site may lead to the true binding mode being inaccessible. This is exemplified by 2CGX, the most flexible ligand used here, where a subtle shift in the glycine rich loop made the experimental binding mode inaccessible. While it is clear that accurate energetics are important, the need to account for protein flexibility is of at least equal importance. The impact of the latter can be minimized by choosing a protein–ligand complex for docking where the ligand is of similar size and/or structure to the lead under investigation,²⁹ or we can restrict the use of QM/MM to systems where conformational effects are less significant. Alternatively, methods such as GLIDE-induced fit,³⁸ or more simulation using methods such as CHARMM,⁵⁵ could be used to explore conformation space. However, both methods have nontrivial computational overheads and lead to larger numbers of structures requiring ranking and are not suitable for high throughput application.

Analysis of the results obtained for the lowest rmsd GOLD solutions reveals that empirical methods such as GOLD and MMFF often generate physically unreasonable ligand conformations, displaying H-bonds to the hinge with unrealistically short H-bonds at ~ 1.4 Å or long at ~ 2.8 Å. In contrast QM/MM based methods are more effective at reproducing the H-bond pattern more observed in the crystal. QM/MM methods can also take into account electron polarization/delocalization effects, which the net +0.1 A.U. charge observed on the lowest rmsd cross-docked poses. These observations collectively help to explain the poor performance of docking programs generally observed in the literature, a result of poor quality structures produced and subsequently scored using poor quality scoring functions.

In summary, these results suggest that the hybrid QM/MM calculations could prove useful as a tool in kinase FBDD. The theoretical scheme used here (MM-docking combined with QM/MM optimization) could prove useful in lead identification by allowing the prediction of a given ligand's binding modes with greater success than traditional MM based methods. In addition, the method provides us with a means to produce accurate, theoretical protein–ligand complexes which give a drug-discovery program team the ability to probe existing interactions between a ligand and protein as well as search for additional new interactions which could prove beneficial in lead optimization. The cost implications are significant since crystallography would only be needed to verify the QM/MM models and assess the impact of protein flexibility when more substantial changes have been made to the lead.

ACKNOWLEDGMENT

M.P.G. would like to thank Drs. Andrew Leach, Mike Hann, Anne Hersey, Paul Bamborough, Joelle Le, Iain McLay, and Colin Edge for their input. D.G. would like to acknowledge the support provided by The Thailand Research Fund.

REFERENCES AND NOTES

- (1) Congreve, M.; Chessari, G.; Dominic Tisi, D.; Woodhead, A. J. Recent Developments in Fragment-Based Drug Discovery. *J. Med. Chem.* **2008**, *51*, 3661–3680.
- (2) Hajduk, P. J.; Greer, J. A decade of fragment-based drug design: strategic advances and lessons learned. *Nat. Rev. Drug Discovery* **2007**, *6*, 211–219.

- (3) Hartshorn, M. J.; Murray, C. W.; Cleasby, A.; Frederickson, M.; Tickle, I. J.; Jhoti, H. Fragment-Based Lead Discovery Using X-ray Crystallography. *J. Med. Chem.* **2005**, *48*, 403–413.
- (4) Hann, M. M.; Leach, A. R.; Harper, G. Molecular complexity and its impact on the probability of finding leads for drug discovery. *J. Chem. Inf. Comput. Sci.* **2001**, *41*, 856–864.
- (5) Jhoti, H.; Cleasby, A.; Verdonk, M.; Williams, G. Fragment-based screening using X-ray crystallography and NMR spectroscopy. *Curr. Opin. Chem. Biol.* **2007**, *11*, 485–493.
- (6) Mooij, W. T. M.; Hartshorn, M. J.; Tickle, I. J.; Sharff, A. J.; Verdonk, M. L.; Jhoti, H. Automated protein-ligand crystallography for structure-based drug design. *Chem. Med. Chem.* **2006**, *1*, 827–838.
- (7) Verdonk, M. L.; Hartshorn, M. J. Structure-guided fragment screening for lead discovery. *Curr. Opin. Drug Discovery Dev.* **2004**, *7*, 404–410.
- (8) Villar, H. O.; Hansen, M. R. Computational techniques in fragment based drug discovery. *Curr. Topics Med. Chem.* **2007**, *7*, 1509–1513.
- (9) Warren, G. L.; Andrews, C. A.; Capelli, A.; Clarke, B.; LaLonde, J.; Lambert, M. H.; Lindvall, M.; Nevins, N.; Semus, S. F.; Senger, S.; Tedesco, G.; Wall, I. D.; Woolven, J. M.; Peishoff, C. E.; Head, M. S. A Critical Assessment of Docking Programs and Scoring Functions. *J. Med. Chem.* **2006**, *49*, 5912–5931.
- (10) Sutherland, J. J.; Nandigam, R. K.; Erickson, J. A.; Veith, M. Lessons in molecular recognition. 2. Assessing and improving cross-docking accuracy. *J. Chem. Inf. Model.* **2007**, *47*, 2293–2302.
- (11) Duca, J. S.; Madison, V. S.; Voigt, J. H. Cross-docking of inhibitors into CDK2 structures 1. *J. Chem. Inf. Model.* **2008**, *48*, 659–668.
- (12) Enyedy, I. J.; Egan, W. J. Can we use docking and scoring for hit-to-lead optimization. *J. Comput.-Aided-Mol. Des.* **2008**, *22*, 161–168.
- (13) Jain, A. N. Bias, reporting, and sharing: computational evaluations of docking methods. *J. Comput.-Aided-Mol. Des.* **2008**, *22*, 201–212.
- (14) Marcou, G.; Rognan, D. Optimizing fragment and scaffold docking by use of molecular interaction fingerprints. *J. Chem. Inf. Model.* **2007**, *47*, 195–207.
- (15) Leach, A. R.; Shoichet, B. K.; Peishoff, C. E. Prediction of Protein-Ligand Interactions. Docking and Scoring: Successes and Gaps. *J. Med. Chem.* **2006**, *49*, 5851–5855.
- (16) Thompson, D. C.; Humblet, C.; McCarthy, D. J. Investigation of MM-PB/SA rescoring of docking poses. *J. Chem. Inf. Model.* **2008**, *48*, 1081–1091.
- (17) Guimaraes, C. R. W.; Cardozo, M. MM-GB/SA rescoring of docking poses in structure-based lead optimization. *J. Chem. Inf. Model.* **2008**, *48*, 958–970.
- (18) Graves, A. P.; Shivakumar, D. M.; Boyce, S. E.; Jacobson, M. P.; Case, A. A.; Shoichet, B. K. Rescoring docking hit lists for model cavity sites: predictions and experimental testing. *J. Mol. Biol.* **2008**, *377*, 914–934.
- (19) Khandelwal, A.; Lukacova, V.; Comez, D.; Kroll, D. M.; Raha, S.; Balaz, S. A combination of docking, QM/MM methods, and MD simulations for binding affinity estimation of metalloprotein ligands. *J. Med. Chem.* **2005**, *48*, 5437–5447.
- (20) Raha, K.; Merz, K. M. large-scale validation of a quantum mechanics based scoring function: predicting the binding affinity and binding mode of a diverse set of protein-ligand complexes. *J. Med. Chem.* **2005**, *48*, 4558–4575.
- (21) Cho, A. E.; Guallar, V.; Berne, B. J.; Friesner, R. Importance of Accurate Charges in Molecular Docking: Quantum Mechanical/Molecular Mechanical (QM/MM) Approach. *J. Comput. Chem.* **2005**, *26*, 915–931.
- (22) Sander, T.; Liljefors, T.; Balle, T. Prediction of the receptor conformation for iGluR2 agonist binding: QM/MM docking to an extensive conformational ensemble generated using normal mode analysis. *J. Mol. Graphics Modell.* **2008**, *26*, 1259–1268.
- (23) GOLD: CCDC, Business & Administration, Cambridge Crystallographic Data Centre, 12 Union Road, Cambridge, CB2 1EZ, UK. <http://www.ccdc.cam.ac.uk> (accessed Feb 18, 2009).
- (24) Friesner, R. A. Combined quantum and molecular mechanics (QM/MM). *Drug Discovery Today* **2004**, *1*, 253–260.
- (25) Manning, G.; Whyte, D. B.; Martinez, R.; Hunter, T.; Sudarsanam, S. The protein kinase complement of the human genome. *Science* **2002**, *298*, 1912–1916.
- (26) Weinmann, H.; Metternich, R. Drug discovery process for kinase inhibitors. *ChemBioChem* **2005**, *6*, 455–459.
- (27) Liao, J. J.-L. Molecular recognition of protein kinase binding pockets for design of potent and selective kinase inhibitors. *J. Med. Chem.* **2007**, *50*, 1–16.
- (28) RCSB Protein databank. <http://www.rcsb.org/> (accessed Feb 18, 2009).
- (29) Verdonk, M. L.; Mortenson, P. N.; Hall, R. J.; Hartshorn, M. J.; Murray, C. W. Protein-Ligand Docking against Non-Native Protein Conformers. *J. Chem. Inf. Model.* **2008**, *48*, 2214–2225.
- (30) Gleeson, M. P.; Gleeson, D. Assessing the utility of hybrid quantum mechanical/molecular mechanical methods in structure-based drug design. *J. Chem. Inf. Model.* **2009**, *49*, xxx.
- (31) Rappe, A. K.; Casewit, C. J.; Colwell, K. S.; Goddard, W. A., III; Skiff, W. M. UFF, a Full Periodic Table Force Field for Molecular Mechanics and Molecular Dynamics Simulations. *J. Am. Chem. Soc.* **1992**, *114*, 10024–10035.
- (32) Dapprich, S.; Komaromi, I.; Byun, K. S.; Morokuma, K.; Frisch, M. J. A new ONIOM implementation in Gaussian98 Part I. The calculation of energies, gradients, vibrational frequencies and electric field derivatives. *J. Mol. Struct.* **1999**, *1–21*, 461–462.
- (33) Vreven, T.; Byun, K. S.; Komaromi, I.; Dapprich, S.; Montgomery, J. A.; Morokuma, K.; Frisch, M. J. Combining Quantum Mechanics Methods with Molecular Mechanics Methods in ONIOM. *J. Chem. Theory Comput.* **2006**, *2*, 815–826.
- (34) Raha, K.; Peters, M. B.; Wang, B.; Yu, N.; Wollacott, A. M.; Westerhoff, L. M.; Merz, K. M. The role of quantum mechanics in structure-based drug design. *Drug Discovery Today* **2007**, *21*, 725–731.
- (35) Lin, H.; Truhlar, D. G. QM/MM: what have we learned, where are we, and where do we go from here. *Theor. Chem. Acc.* **2007**, *117*, 185–199.
- (36) Halgren, T. A. Merck Molecular Force Field. I. Basis, Form, Scope, Parameterization, and Performance of MMFF94. *J. Comput. Chem.* **1996**, *5&6*, 490–519.
- (37) Bostrom, J.; Hogner, A.; Schmitt, S. Do structurally similar molecules bind in a similar fashion. *J. Med. Chem.* **2006**, *49*, 6716–6725.
- (38) Schrodinger, Dynamostasse 13, D-68165 Mannheim, Germany. www.schrodinger.com (accessed Feb 18, 2009).
- (39) Frisch, M. J.; Trucks, G. W.; Schlegel, H. B.; Scuseria, G. E.; Robb, M. A.; Cheeseman, J. R.; Montgomery, J. A., Jr.; Vreven, T.; Kudin, K. N.; Burant, J. C.; Millam, J. M.; Iyengar, S. S.; Tomasi, J.; Barone, V.; Mennucci, B.; Cossi, M.; Scalmani, G.; Rega, N.; Petersson, G. A.; Nakatsuji, H.; Hada, M.; Ehara, M.; Toyota, K.; Fukuda, R.; Hasegawa, J.; Ishida, M.; Nakajima, T.; Honda, Y.; Kitao, O.; Nakai, H.; Klene, M.; Li, X.; Knox, J. E.; Hratchian, H. P.; Cross, J. B.; Bakken, V.; Adamo, C.; Jaramillo, J.; Gomperts, R.; Stratmann, R. E.; Yazyev, O.; Austin, A. J.; Cammi, R.; Pomelli, C.; Ochterski, J. W.; Ayala, P. Y.; Morokuma, K.; Voth, G. A.; Salvador, P.; Dannenberg, J. J.; Zakrzewski, V. G.; Dapprich, S.; Daniels, A. D.; Strain, M. C.; Farkas, O.; Malick, D. K.; Rabuck, A. D.; Raghavachari, K.; Foresman, J. B.; Ortiz, J. V.; Cui, Q.; Baboul, A. G.; Clifford, S.; Cioslowski, J.; Stefanov, B. B.; Liu, G.; Liashenko, A.; Piskorz, P.; Komaromi, I.; Martin, R. L.; Fox, D. J.; Keith, T.; Al-Laham, M. A.; Peng, C. Y.; Nanayakkara, A.; Challacombe, M.; Gill, P. M. W.; Johnson, B.; Chen, W.; Wong, M. W.; Gonzalez, C.; Pople, J. A. *Gaussian 03, Revision C.02*; Gaussian, Inc.: Wallingford, CT, 2004.
- (40) Bultinck, P.; Langenaeker, W.; Lahorte, P.; De Proft, F.; Geerlings, P.; Waroquier, M.; Tollenaere, J. P. The Electronegativity Equalization Method I: Parametrization and Validation for Atomic Charge Calculations. *J. Phys. Chem. A* **2002**, *106*, 7887–7894.
- (41) Rappe, A. K.; Casewit, C. J.; Colwell, K. S.; Goddard, W. A., III; Skiff, W. M. UFF, a Full Periodic Table Force Field for Molecular Mechanics and Molecular Dynamics Simulations. *J. Am. Chem. Soc.* **1992**, *114*, 10024–10035.
- (42) Namuangruk, S.; Khongpracha, P.; Pantu, P.; Limtrakul, J. Structures and Reaction Mechanisms of Propene Oxide Isomerization on H-ZSM-5: An ONIOM Study. *J. Phys. Chem. B* **2006**, *110*, 25950–25957.
- (43) Namuangruk, S.; Tantanak, D.; Limtrakul, J. Application of ONIOM calculations in the study of the effect of the zeolite framework on the adsorption of alkenes to ZSM-5. *J. Mol. Catal. A: Chem.* **2006**, *256*, 113–121.
- (44) Jungsuttiwong, S.; Limtrakul, J.; Truong, T. N. Theoretical Study of Modes of Adsorption of Water Dimer on H-ZSM-5 and H-Faujasite Zeolites. *J. Phys. Chem. B* **2005**, *109*, 13342–13351.
- (45) Bathelt, C. M.; Mulholland, A. J.; Harvey, J. N. QM/MM Modeling of Benzene Hydroxylation in Human Cytochrome P450 2C9. *J. Phys. Chem. A* **2008**, *112*, 13149–13156.
- (46) Halgren, T. A. Merck Molecular Force Field. I. Basis, Form, Scope, Parameterization, and Performance of MMFF94. *J. Comput. Chem.* **1996**, *5&6*, 490–519.
- (47) Molecular Operating Environment: Chemical Computing Group, 1010 Sherbrooke St. W, Suite 910 Montreal, Quebec, Canada H3A 2R7. www.cchemcomp.com (accessed Feb 18, 2009).
- (48) Cornell, W. D.; Cieplak, P.; Bayly, C. I.; Gould, I. R.; Merz, K. M.; Ferguson, D. M.; Spellmeyer, D. C.; Fox, T.; Caldwell, J. W.; Kollman, P. A. A Second Generation Force Field for the Simulation of Proteins, Nucleic Acids, and Organic Molecules. *J. Am. Chem. Soc.* **1995**, *117*, 5179–5197.
- (49) MacKerell, A. D., Jr.; Bashford, D.; Bellott, M.; Dunbrack, R. L., Jr.; Evanseck, J. D.; Field, M. J.; Fischer, S.; Gao, J.; Guo, H.; Ha, S.; Joseph-McCarthy, D.; Kuchnir, L.; Kuczera, K.; Lau, F. T. K.; Mattos, C.; Michnick, S.; Ngo, T.; Nguyen, D. T.; Prodhom, B.; Reiher, W. E.,

- III; Roux, B.; Schlenkrich, M.; Smith, J. C.; Stote, R.; Straub, J.; Watanabe, M.; Wiorkiewicz-Kuczera, J.; Yin, D.; Karplus, M. All-Atom Empirical Potential for Molecular Modeling and Dynamics Studies of Proteins. *J. Phys. Chem. B* **1998**, *102*, 3586–3616.
- (50) Yusuf, D.; Davis, A. M.; Kleywegt, G. J.; Schmitt, S. An Alternative Method for the Evaluation of Docking Performance: RSR vs RMSD. *J. Chem. Inf. Model.* **2008**, *48*, 1411–1422.
- (51) Kleywegt, G. J.; Jones, T. A. Good Model-building and Refinement Practice. *Methods Enzymol.* **1997**, *277*, 208–230.
- (52) Bostrom, J. Reproducing the conformations of protein-bound ligands: A critical evaluation of several popular conformational searching tools. *J. Comput.-Aided Mol. Des.* **2001**, *15*, 1137–1152.
- (53) Yusuf, D.; Davis, A. M.; Kleywegt, G. J.; Schmitt, S. An Alternative Method for the Evaluation of Docking Performance: RSR vs RMSD. *J. Chem. Inf. Model.* **2008**, *48*, 1411–1422.
- (54) Warshel, A. Electrostatic Origin of the Catalytic Power of Enzymes and the Role of Preorganized Active Sites. *J. Biol. Chem.* **1998**, *273*, 27035–27038.
- (55) Brooks, B. R.; Bruccoleri, R. E.; Olafson, B. D.; States, D. J.; Swaminathan, S.; Karplus, M. CHARMM: A Program for Macromolecular Energy, Minimization, and Dynamics Calculations. *J. Comput. Chem.* **1983**, *4*, 187–217.

CI900022H